Spacetime Embedding Diagrams for Ramond-Ramond p-Branes in String Theory

Abel Shiferaw*

School of Physics, Georgia Institute of Technology, Atlanta, GA 30332, USA

Don Marolf (REU Mentor)†

Department of Physics, University of California, Santa Barbara, CA 93106, USA

(Dated: October 1, 2021)

It has previously been observed that it is possible to embed the rt-plane of the maximally extended Schwarzschild black hole into $2+1$ Minkowski space [1]. The construction was later on generalized to other spherically symmetric black holes with multiple horizons [2]. This paper further generalizes the construction to the class of Ramond-Ramond (R-R) p-branes in string theory. In particular, we illustrate how to construct spacetime embedding diagrams for the non-extreme Ramond-Ramond (R-R) p-branes and discuss features of the resulting diagram for the $p=6$ case. We then explore the behavior of the embedding diagrams at extremality for various choices of p.

I. INTRODUCTION

Embedding diagrams are an indispensable aid for visualizing curved spaces. A famous example in general relativity (GR) is the Einstein-Rosen bridge, which describes two asymptotically flat regions connected together by a black hole; see FIG. 1. The resulting diagram illustrates the spatial curvature of constant time slices for the eternal Schwarzschild black hole, among other features.

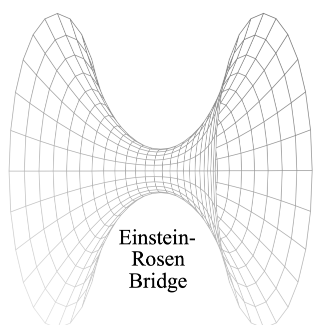

FIG. 1. The $r\varphi$-plane of the eternal Schwarzschild black hole.

An alternative approach is to construct diagrams by embedding the rt-plane of a given *spacetime* into $2+1$ Minkowski space [1,2]. This construction provides a way to discuss the spacetime curvature, a fundamental feature of Einstein's theory of gravity, and its higher-dimensional generalizations such as string theory. The purpose of this paper is to utilize this technique to construct spacetime embedding diagrams for the R-R p-brane solutions of string theory [3].

The R-R p-brane solutions are interesting for several reasons. Perhaps most importantly, in their extremal limit, these objects play an essential role in describing D-branes, which are the fundamental ingredients of string theory [4]. This relationship, in turn, has led to a landmark discovery involving a microscopic description of the Bekenstein-Hawking entropy formula [5]

$$S_{BH} = \frac{\text{Area}_H}{4G_N}, \tag{1}$$

where G_N is Newton's gravitational constant. Thus, given the importance of the R-R p-brane solutions to theoretical physics, it is important to have a better visual understanding of their properties that can be used to aid students and experts alike.

The outline of the paper is as follows. In section II, we discuss the properties of the R-R p-brane solutions. In section III, we outline the embedding construction for the non-extreme cases. In section IV, after presenting our general formalism, we specialize in the case of $p=6$ and discuss the basic features of the resulting embedding diagram. In section V, we show that it is possible to embed a region near the extremal 4-brane and 5-brane into $2+1$ Minkowski space. We end with conclusions and outlook in section VI.

II. R-R p-BRANE SOLUTIONS

In the so-called string conformal frame, the non-extreme R-R p-brane solutions are [3]

$$\begin{aligned} \mathrm{d}s^2 = &\frac{1}{\sqrt{H(r)}}\bigg(-f(r)\,\mathrm{d}t^2 + \sum_{i=1}^{p}(\mathrm{d}x^i)^2\bigg) \\ &+ \sqrt{H(r)}\bigg(\frac{\mathrm{d}r^2}{f(r)} + r^2\mathrm{d}\Omega_{8-p}^2\bigg), \end{aligned} \tag{2}$$

where

$$H(r) = 1+\sinh^2\alpha\left(\frac{r_0}{r}\right)^{7-p}, \quad f(r) = 1-\left(\frac{r_0}{r}\right)^{7-p}, \tag{3}$$

$\mathrm{d}\Omega_{8-p}^2$ denotes the round metric on $\mathbb{S}^{8-p}$, and x_i are spatial coordinates along the brane. Here t is the coordinate time, and it represents the time measured by

* ashiferaw6@gatech.edu

† marolf@physics.ucsb.edu

an observer at spatial infinity. The coordinate r is the radial coordinate and is defined so that the area of $\mathbb{S}^{8-p}$ at r is $\frac{2\pi^{\frac{9-p}{2}}}{\Gamma\left(\frac{9-p}{2}\right)} r^{8-p}$. We focus on the cases $p < 7$, since we are interested in asymptotically flat solutions in 10 dimensions.

The radius r_0 is called the *event horizon*. The metric appears to be singular at $r = r_0$, but this is merely a consequence of a poor choice of coordinates. At this location, the signs for the coefficient of dt^2 and dr^2 interchange in eq. (2). The coordinate r becomes timelike, and an observer inside the horizon ($r < r_0$) will have to travel faster than the speed of light to stay at the same radius. At $r = 0$, we have a *singularity*. The size of $\mathbb{S}^{8-p}$ contracts to zero, and the metric diverges.

Our solution is parameterized by the two independent quantities: r_0, and α. These may be traded for the mass M per unit $p-$volume V_p, and charge Q

$$M/V_p = \frac{\pi^{\frac{9-p}{2}}(8-p)}{\Gamma\left(\frac{9-p}{2}\right)} r_0^{7-p} \left(1 + \frac{7-p}{8-p}\sinh^2\alpha\right), \qquad (4)$$

$$Q = \frac{\pi^{\frac{9-p}{2}}(7-p)}{\Gamma\left(\frac{9-p}{2}\right)} r_0^{7-p} \sinh\alpha\cosh\alpha, \qquad (5)$$

where $\alpha = [0, \infty)$ is the parameter that controls how close we are to extremality. More precisely, the extremal limit ($M \to Q$) occurs when $\alpha \to \infty$ and $r_0 \to 0$ ($f(r) \to 1$) with $r_0^{7-p}\sinh 2\alpha$ held fixed.

It will be useful to understand the division of the R-R spacetime for our construction in section III. This is best captured with a Penrose diagram; see FIG. 2. We see that the global structure is similar to the familiar Schwarzschild solution except that each point now represents $\mathbb{R}^p \times \mathbb{S}^{8-p}$.[1]

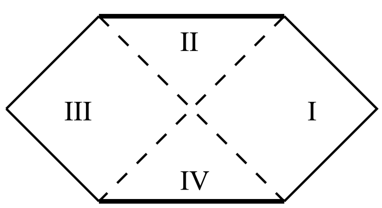

FIG. 2. The Penrose diagram for the non-extreme R-R p-branes. Ingoing and outgoing dotted lines represent light rays traveling at 45°, solid black lines represent the various infinities that are conformally rescaled, and heavy black lines represent the future and past singularities. Regions I and III correspond to the exterior regions, while regions II and IV represent the two copies of the interior regions.

[1] One might expect the global structure to be similar to the Reissner–Nordström spacetime since our p-branes are charged under $p+1$ form gauge potentials. However, introducing the dilaton field in low energy string theory changes the causal structure, making them more like Schwarzschild. Indeed, we will see that our embedding diagram is not much different from the Schwarzschild case [6].

III. CONSTRUCTION

We follow closely the technique outlined in [1] for the eternal Schwarzschild black hole. This section only addresses the embedding process for region I ($r > r_0$). The construction for the other regions is similar, except for a few minus signs.

We start by considering the rt-plane ($\mathrm{d}x^i = \mathrm{d}\Omega_{8-p} = 0$)

$$\mathrm{d}s^2 = -\frac{f(r)}{\sqrt{H(r)}}\mathrm{d}t^2 + \frac{\sqrt{H(r)}}{f(r)}\mathrm{d}r^2, \qquad (6)$$

where $H(r)$ and $f(r)$ are defined in section II. It is important to note that the reduced metric contains a time translation symmetry $t \to t + \delta t$ inherited from the original spacetime. This suggests that it should be possible to embed the slice as a hyperbolic surface into $2+1$ Minkowski space with metric

$$\mathrm{d}s^2 = -\mathrm{d}T^2 + \mathrm{d}X^2 + \mathrm{d}Y^2. \qquad (7)$$

The time translation symmetry is related to a boost symmetry near the point where the past and future horizons intersect in $1+1$ Minkowski space. In light of this, we introduce coordinates adapted to the boost symmetry

$$T = \rho\sinh\varphi \quad \text{and} \quad X = \rho\cosh\varphi, \qquad (8)$$

after which eq. (7) becomes

$$\mathrm{d}s^2 = -\rho^2\mathrm{d}\varphi^2 + \mathrm{d}\rho^2 + \mathrm{d}Y^2. \qquad (9)$$

To understand the behavior near the aforementioned surface, we define

$$r = r_0 + \eta, \qquad (10)$$

where $r_0 \gg \eta$. We further assume that $\eta > 0$, since we are working in the region outside the future horizon. To order η, eq. (6) becomes

$$\mathrm{d}s^2 \cong -\frac{(7-p)\eta}{r_0\cosh\alpha}\mathrm{d}t^2 + \frac{r_0\cosh\alpha}{(7-p)\eta}\mathrm{d}\eta^2. \qquad (11)$$

The metric is singular at $\eta = 0$, but this is just an artifact of our choice of coordinates. This problem can be circumvented by introducing a tortoise-like radial coordinate χ that measures proper distance

$$\eta = \frac{7-p}{4r_0\cosh\alpha}\chi^2, \qquad (12)$$

so that

$$\mathrm{d}s^2 \cong -\frac{(7-p)^2}{4r_0^2\cosh^2\alpha}\chi^2\mathrm{d}t^2 + \mathrm{d}\chi^2. \qquad (13)$$

Now, in order for the above metric to agree with eq. (9), we need to set

$$\rho = \chi \quad \text{and} \quad \varphi = \frac{7-p}{2r_0\cosh\alpha}t. \qquad (14)$$

Having matched the near-horizon region of the R-R spacetime to $1+1$ Minkowski space, we now turn to extend the symmetry to the entire spacetime. The killing fields can be easily related

$$\partial_\varphi = \frac{7-p}{2r_0\cosh\alpha}\partial_t. \tag{15}$$

We can compute the norm from eq. (9) and eq. (6), and equate and solve for ρ

$$\rho = \frac{2r_0\cosh\alpha\sqrt{\frac{1-\left(r_0/r\right)^{7-p}}{\sqrt{1+\sinh^2\alpha\left(r_0/r\right)^{7-p}}}}}{7-p}. \tag{16}$$

To conclude our construction, we need to give Y as a function of r and t. But, by symmetry, Y must only depend on r, since eq. (6) enjoys a time translation symmetry. We can then solve for $Y(r)$ by demanding the metrics to agree on a $t=$ const. time slice

$$\frac{\sqrt{H(r)}}{f(r)}\mathrm{d}r^2 = \mathrm{d}\rho^2 + \mathrm{d}Y^2. \tag{17}$$

Performing this calculation in *Mathematica*, we find

$$Y(r) = \int_{r_0}^{r}\mathrm{d}r\sqrt{\frac{4\left(1+\sinh^2\alpha\left(r_0/r\right)^{7-p}\right)^3 - r_0^{16-4p}r^{2p-30}\cosh^2\alpha\left(2r_0^pr^7+\sinh^2\alpha\left(r_0^pr^7+r_0^7r^p\right)\right)^2}{4\left(1-\left(r_0/r\right)^{7-p}\right)\left(1+\sinh^2\alpha\left(r_0/r\right)^{7-p}\right)^{5/2}}}. \tag{18}$$

IV. EMBEDDING DIAGRAM

We will now briefly review the basic features of our spacetime embedding diagram. A much thorough review for the Schwarzschild black hole can be found in [1]. Without loss of generality, we will focus on the case $p=6$. There is nothing special per se about our choice; the explanations generalize trivially for $p<6$. The choice was particularly made to simplify the discussion, since when $p=6$, the metric on $\mathbb{S}^{8-p}$ becomes $\mathbb{S}^2$, which is easy to visualize. The embedding diagram for the non-extreme 6-brane is given in FIG. 3.

Perhaps the first thing to note about the non-extreme 6-brane solution is that it is asymptotically flat, i.e., as $r\to\infty$, the metric tends to Minkowski space in spherical coordinates

$$\mathrm{d}s^2 = -\mathrm{d}t^2 + \sum_{i=1}^{6}(\mathrm{d}x^i)^2 + \mathrm{d}r^2 + r^2\mathrm{d}\Omega_2^2. \tag{19}$$

This property can be readily visualized by considering the lines on our embedding diagram. The two flanges correspond to the two asymptotic regions (regions I and III). If we choose any one of the lines that are drawn to guide our eyes, we see that they become straighter and straighter. Thus, our diagram is only curved in one direction (XT plane), and curvature in one direction does not change the intrinsic geometry of the R-R geometry.

Another important feature of our spacetime is the horizon, and much of the interesting physics of black holes and branes rests in understanding what happens here. One could, for example, use our diagram to look at outward directed light rays from an infalling observer. This can be used to determine that the black lines that separate the different regions are null rays. In other words, the horizon on our diagram is made up of light rays that are trying to escape but never make any progress since they stay at $Y=0$.

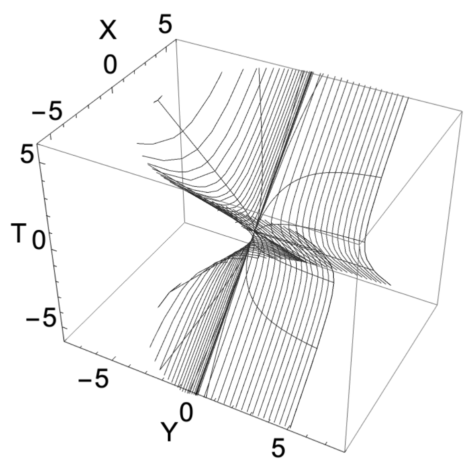

FIG. 3. The spacetime embedding diagram for the non-extreme R-R 6-brane with $r_0=1$, and $\alpha=0$. The vertical direction T is timelike, and the horizontal directions (X and Y) are spacelike. The black lines on our diagram represent light rays moving at 45° everywhere with respect to the T axis.

A final feature manifest on our diagram is the singularity. The singularity is located at a Minkowski time coordinate $T=\pm\infty$. This is due to the boost-like nature of the time translation symmetry of the R-R spacetime. We can see that outside the black brane, the symmetry is timelike, which means that the surface is not changing with time. However, inside, the symmetry is spacelike, and thus the interior regions vary with time.

There is a natural question that arises with the location of the singularity. If the singularity is to be located at $T = \pm\infty$, then does it imply that an infalling observer takes an infinite time to reach the singularity? The answer is no. The infalling observer naturally measures proper time along their worldline, and this turns out to be finite at the past and future timelike infinity. This is associated with the fact that the interior surface follows a light cone in Minkowski space, so the whole surface moves at the speed of light, which accounts for why a short amount of proper time elapses.

V. EXTREMAL p-BRANES

We now turn to studying the extremal limit in which $r_0 \to 0$. In the vicinity of the horizon ($r = 0$), the constant term in $H(r)$ may be ignored. The resulting near-horizon metric simplifies to

$$\mathrm{d}s^2 = -\left(\frac{r}{L}\right)^{\frac{7-p}{2}} \mathrm{d}t^2 + \left(\frac{L}{r}\right)^{\frac{7-p}{2}} \mathrm{d}r^2, \tag{20}$$

with $L^{7-p} = r_0^{7-p} \sinh^2\alpha$. For $p > 3$, we introduce the tortoise coordinate

$$\sigma = \frac{4r^{\frac{p-3}{4}} L^{\frac{7-p}{4}}}{p-3}, \tag{21}$$

so that

$$\mathrm{d}s^2 = -\ell^2\sigma^{2\gamma}\mathrm{d}t^2 + \mathrm{d}\sigma^2, \tag{22}$$

with $\ell = \left(\frac{p-3}{4L}\right)^\gamma$ and $\gamma = \frac{7-p}{p-3}$. A quick comparison with eq. (9) suggests setting $\varphi = \beta t$ for $\beta \in \mathbb{R}$. Then, it follows that

$$\rho = \frac{\ell}{\beta}\sigma^\gamma. \tag{23}$$

Furthermore, for $\sigma < (\frac{\beta}{\ell\gamma})^{1/(\gamma-1)}$, we can solve for $Y(\sigma)$ by using

$$Y(\sigma) = \int_0^\sigma \mathrm{d}\sigma\sqrt{1 - \left(\frac{\ell\gamma}{\beta}\right)^2 \sigma^{2(\gamma-1)}}. \tag{24}$$

Now, let's consider the case of $p = 4$, which gives $\gamma = 3$ and $\ell = (4L)^3$. In particular, $\rho \sim \sigma^4 \sim r^{1/4}$, so the horizon at $r = 0$ is also at $\sigma = 0$, and thus $\rho = 0$, as desired. In terms of r, eq. (24) becomes

$$Y(r) = \int_0^r \mathrm{d}r\sqrt{\left(\frac{L}{r}\right)^{3/2} - \frac{9}{16\beta^2L^3\sqrt{r}}}. \tag{25}$$

Thus, we can indeed embed the region near the extreme 4-brane into $2+1$ Minkowski space; see FIG. 4.

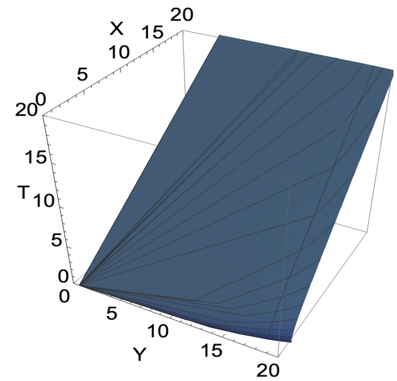

FIG. 4. The embedding diagram for the extreme 4-brane with $L = 4$ and $\beta = 1$.

Proceeding similarly for the case of $p = 5$, one arrives at the following embedding equation for $Y(r)$

$$Y(r) = \frac{\sqrt{4\beta^2L^2 - 1}}{2\beta\sqrt{L}} \int_0^r \frac{\mathrm{d}r}{\sqrt{r}}. \tag{26}$$

The embedding diagram is shown in FIG. 5.

In contrast, the analogous approach fails for $p = 6$ because $1 - \left(\frac{\ell\gamma}{\beta}\right)^2 \sigma^{2(\gamma-1)}$ is negative near the horizon. This may well be related to the fact that the singularity is timelike for $p = 6$. For $p \leq 3$, one finds $\sigma \to \infty$ at the horizon. Thus, they cannot be embedded in the above way in $2+1$ Minkowski space.

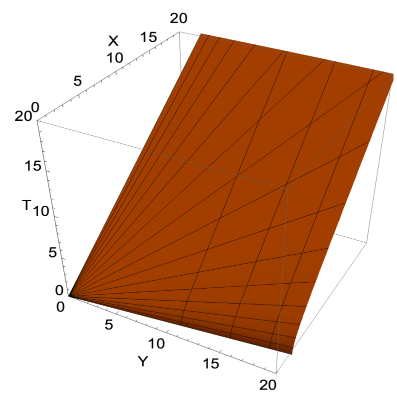

FIG. 5. The embedding diagram for the extreme 5-brane with $L = 4$ and $\beta = 1$.

VI. CONCLUSION

We have showed that it is possible to embed the non-extreme R-R p-brane solutions into $2+1$ Minkowski space for all values of $p \leq 6$. We also studied the extremal versions of the R-R p-brane solutions and showed that one could embed a region for $p = 4, 5$. We also noted that our construction fails for the case of $p \leq 3$, a feature that is not manifest in the non-extreme cases.

In the future, it would be interesting to go back to the $p = 4, 5$ cases and understand what happens when we include $f(r)$ in the extremal metric. One can also ask if there exists a different embedding that would work for $p = 6$. Since the singularity there is timelike, one might expect to use a more standard Minkowski coordinates T, X, Y in terms of which the Minkowski metric is

$$\mathrm{d}s^2 = -\mathrm{d}T^2 + \mathrm{d}X^2 + \mathrm{d}Y^2. \tag{27}$$

ACKNOWLEDGMENTS

I want to thank my advisor, Professor Don Marolf, for crafting a pedagogical project, allowing me to learn as much as I can during the summer, providing clear explanations, and inspiring my interest in learning more about black holes and string theory. I would also like to thank my graduate mentors, Molly Kaplan and Zhencheng Wang, for answering my questions with Mathematica, general relativity, and graduate programs. Lastly, thank you to Dr. Sathya Guruswamy, the UCSB REU site director, for coordinating the events, supporting the REU cohort with professional development activities, and mentoring us in every imaginable way possible. In addition, I would like to thank the national science foundation for supporting this work and allowing me and other students to hone research experience during the summer. This work was supported by NSF REU grant PHY-1852574.

[1] Donald Marolf. Spacetime Embedding Diagrams for Black Holes, *Gen. Rel. Grav.* ***31****, 919 (1999), arXiv:9806123[gr-qc], 1998.*

[2] Giblin Jr, J.T.; Marolf, D.; Garvey, R.H. Spacetime Embedding Diagrams for Spherically Symmetric Black Holes. *Gen. Rel. Grav. 2004, 36, 83–99, [arXiv:gr-qc/0305102].*

[3] G. Horowitz and A. Strominger, *Black strings and P-branes*, Nucl. Phys. B **360**, 197-209 (1991) doi:10.1016/0550-3213(91)90440-9

[4] J. Polchinski, *Dirichlet Branes and Ramond-Ramond charges, Phys. Rev. Lett.* ***75****, [arXiv:hep-th/9510017*, 1995.

[5] A. Strominger and C. Vafa, *Microscopic origin of the Bekenstein-Hawking entropy, Phys. Lett. B* ***379****, 99-104, [arXiv:hep-th/9601029]*, 1996.

[6] G.Gibbons and K.Maeda, Nucl. Phys. B**298** 741 (1988).